Hybrid Ultrawideband Modulations Compatible for Both Coherent and Transmit-Reference Receivers

Shiwei Zhao, Philip Orlik, Andreas Molisch, Huaping Liu, Jinyun Zhang

Abstract

This paper considers signaling schemes for heterogeneous ultrawideband communications networks that contain both coherent (rake) and transmitted-reference (TR) receivers. While coherent receivers are capable of receiving TR signals, they do so with a 3 dB penalty, because they cannot make use of the energy invested into the reference pulse. We propose a new signaling scheme that avoids this drawback, by encoding redundant information on the reference pulse. The resulting scheme does not affect the operation of a TR receiver, while recovering the 3 dB penalty and furthermore providing an additional 1.7 dB coding gain to a coherent uncoded binary scheme. This can be explained by interpreting the scheme as a trellis-coded modulation. We also provide an alternative implementation that can be viewed as a recursive systematic convolutional encoder. Combining this version further with a simple forward error correction encoder results in a concatenated code that can be decoded iteratively, providing a bit-error rate of 10-3 at 2.8 dB signal-to-noise ratio in additive white Gaussian noise. The convergence behavior of this iterative code is analyzed by using extrinsic information transfer charts.

Hybrid Ultrawideband Modulations Compatible for Both Coherent and Transmit-Reference Receivers

Shiwei Zhao, Philip Orlik, *Member, IEEE*, Andreas F. Molisch, *Fellow, IEEE*, Huaping Liu, *Member, IEEE*, and Jinyun Zhang

Abstract— This paper considers signaling schemes for heterogeneous ultrawideband communications networks that contain both coherent (rake) and transmitted-reference (TR) receivers. While coherent receivers are capable of receiving TR signals, they do so with a 3 dB penalty, because they cannot make use of the energy invested into the reference pulse. We propose a new signaling scheme that avoids this drawback, by encoding redundant information on the reference pulse. The resulting scheme does not affect the operation of a TR receiver, while recovering the 3 dB penalty and furthermore providing an additional 1.7 dB coding gain to a coherent uncoded binary scheme. This can be explained by interpreting the scheme as a trellis-coded modulation. We also provide an alternative implementation that can be viewed as a *recursive* systematic convolutional encoder. Combining this version further with a simple forward error correction encoder results in a concatenated code that can be decoded iteratively, providing a bit-error rate of 10^{-3} at 2.8 dB signal-to-noise ratio in additive white Gaussian noise. The convergence behavior of this iterative code is analyzed by using extrinsic information transfer charts.

Index Terms— Coherent rake, EXIT chart, iterative decoding, recursive systematic convolutional code, transmit-reference, ultrawideband.

I. INTRODUCTION

ULTRAWIDEBAND (UWB) communications systems have become popular for sensor networks because of their good immunity to fading, good multiple-access properties, and possibility of obtaining accurate ranging and geolocation [1]–[4]. Impulse radio (IR), which represents each symbol by one or a sequence of short pulses [5], [6] is the modulation/multiple access method of choice for sensor networks. For example, it is used in the baseline draft for the emerging IEEE 802.15.4a standard for wireless sensor networks.

One of the key challenges for impulse radio is the construction of low-cost receivers that work well in multipath environments. Optimum performance is obtained by a coherent rake receiver that has enough fingers to receive all

resolvable multipath components (MPCs) [7], [8]. However, the number of MPCs can be on the order of tens or even hundreds in typical indoor environments (see [9]–[11] and references therein). Though simplified rake structures have been proposed [12], channel estimation, multipath tracking, and multipath combining contribute to the overall complexity of coherent rake receivers.

For these reasons, transmitted-reference (TR) receivers have drawn significant attention in recent years [13]–[18]. TR encodes the data in the phase difference of the two pulses of a pulse pair. The first pulse in that pair does not carry information, but serves as a reference pulse; the second pulse is modulated by the data and is referred to as the data pulse. The two pulses are separated by a fixed delay. It can be easily shown that the receiver can demodulate this signal by simply multiplying the received signal with a delayed version of itself[1]. TR receivers are thus exceedingly simple, but they show considerably worse performance than coherent rake receivers.

Users in a UWB network often have different quality of service (QoS) requirements. It is thus very desirable to enable a heterogeneous network structure, where users can flexibly choose the type of receiver sufficient to achieve their specific QoS targets while minimizing cost. This requires a "universal" modulation method compatible with different types of receivers such as coherent rake and TR receivers. Technically, it is possible to demodulate TR signals with a coherent receiver, by simply "throwing away" the reference pulses. However, this implies a 3 dB signal energy penalty compared to a system that is designed to use coherent receivers only. On the other hand, signals designed for coherent receivers (i.e., those without reference pulses) obviously cannot be demodulated by a TR receiver.

We propose a hybrid modulation method that enables coherent rake receivers and TR receivers in the same wireless network to simultaneously receive the signal with high quality. The key idea here is to make the "reference pulse" information bearing, without modifying the phase relationship between the reference pulse and data pulse which is critical for the TR receiver operation. This makes sure that the energy in the reference pulse is not "wasted" for the coherent receiver, and recovers the 3 dB loss by "normal" TR signaling. Furthermore, we let the information in the reference pulse

---

[1]Note that the scheme is different from the differential modulation, where data are encoded in the phase difference between successive *symbols*. Differential modulation is not practical for low-data-rate UWB signals, due to the long duration of the required delays.

depend on the *previous* information symbol. Specifically, we let the absolute phase of the reference pulse in the current bit depend on the previous data bit, and the current data bit determines the phase/polarity difference between the reference pulse and the data pulse. This introduces memory into the modulation, which leads to a further performance gain: it is effectively a form of trellis coded modulation (TCM), which enables coherent receivers to achieve better performance than memoryless linear modulation techniques (e.g., bipolar) by taking advantage of this memory through detectors such as a maximum likelihood sequence detector (MLSD). It should be mentioned that the proposed signaling scheme is applicable not only to pulsed UWB systems, but also to narrowband or conventional spread spectrum systems.

The proposed hybrid modulation scheme also offers great advantages when combined further with forward error correction (FEC). The hybrid modulation scheme can be interpreted as a convolutional code with a short constraint length. By viewing FEC combined with hybrid modulation as a form of concatenated coding, this perspective allows us to apply iterative decoding techniques in the receiver, resulting in performance improvements comparable to serially or parallel concatenated coding schemes. A key advantage over serially/parallel concatenated codes is that it does not have the extra complexity or data rate loss caused by the additional FEC code. Still, the design methodology developed for traditional concatenated codes such as turbo codes can be conveniently applied to optimize the design of the constituent encoders [19], [21], [22]. For these purposes, we propose to transform the hybrid modulation, which can be viewed as a non-recursive systematic code, into a recursive code, which is favored by iterative decoding methods. We thus also propose a modified, recursive modulation format, which will work better by employing iterative decoding and can still be demodulated by TR receivers.

The rest of the paper is organized as follows. Section II presents the details of the basic hybrid system. Section III describes the application of iterative decoding and the modified modulation format for performance improvement. The technique of extrinsic information transfer (EXIT) charts [21], [22] is used in Section IV to predict the performance of iterative decoders with the two proposed modulation formats. Section V provides simulation results for the proposed system, followed by conclusions in Section VI.

II. A HYBRID UWB TRANSMISSION SCHEME

A. Basic Idea

In the proposed scheme, whose basic idea can be found in [23], each bit or symbol is represented by N_f pulse pairs, where N_f is a positive integer. The two pulses in each pair are separated by a fixed time T_d. The symbol duration - the time it takes to transmit a bit/symbol - is T_s. Each symbol period is partitioned into N_f frames, each of duration T_f. Each frame is partitioned into N_c chips, each of duration T_c, which typically corresponds to a pulse period. The three quantities T_s, T_f, and T_c satisfy the following relationship:
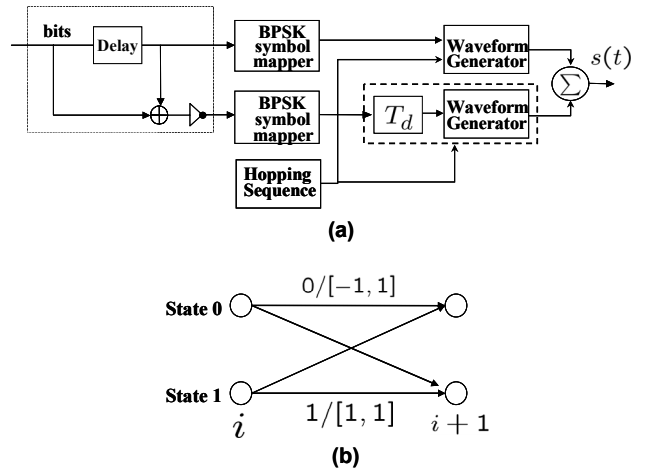
$$T_s = N_f T_f = N_f N_c T_c. \tag{1}$$

Fig. 1. (a) Block diagram of the hybrid transmitter; (b) Trellis representation of the hybrid modulation.

Time-hopping (TH) and polarity scrambling are applied on each symbol to obtain processing gain, to combat multiple-access interference (MAI), and to smooth the signal spectrum. Specifically, each pulse pair is delayed by a pseudorandom time [6], and multiplied with a pseudorandom polarity scrambling that can take on the values ± 1 [24]; this can be easily undone at the receiver.

We now consider the mathematical formulation of an arbitrary signal that can be received by a TR receiver. We write this signal in a form that will turn out to be especially suitable for our later discussion:

$$s_{TX}(t) = \sqrt{\frac{E_s}{2N_f}} \sum_{j=-\infty}^{\infty} d_j \left[(2\beta_j - 1)p(t - jT_f - c_jT_c) + \right.$$
$$\left. \left(2(\overline{\beta_j \oplus b_{\lfloor j/N_f - 1 \rfloor}}) - 1\right) p(t - jT_f - c_jT_c - T_d) \right] \tag{2}$$

where b_i is the i-th information bit, $i = \lfloor j/N_f \rfloor$, $\lfloor \cdot \rfloor$ denotes the integer part, E_s is the bit/symbol energy, $p(t)$ is the short-duration UWB pulse shape whose energy is normalized to $E_p = \int_{-\infty}^{\infty} p^2(t)dt = 1$, and $d_j \in \{-1, 1\}$ is an optional polarity scrambling sequence applied to each pulse pair of the transmitted signal to smooth the signal spectrum. If the system uses an FEC, then $\{b_i\}$ are the outputs of the FEC encoder. The $c_j \in \{0, 1, ..., N_{TH}\}$ constitutes the j-th entry of the TH sequence for the user under consideration. The TH code must satisfy $N_{TH} < N_c$ and $N_c T_c = N_{TH} T_c + T_d + T_g$, where T_g is a guard time set to protect information signals from inter-frame interference. In order to provide the most general formulation, we have also introduced a polarity encoding β_j. To our knowledge all previous publications on TR set $\beta_j = 1$.

As mentioned in the introduction, the key idea of our hybrid modulator is to transmit redundant information on the reference pulses, in other words, to make the β_j dependent on the information symbols:

$$\beta_j = b_{\lfloor j/N_f \rfloor - 1}. \tag{3}$$

Fig. 1(a) shows a block diagram of the transmitter that realizes the above waveform.

Table I shows the four possible combinations of two consecutive bits, the corresponding values of the reference and data

TABLE I
INPUT AND OUTPUT COMBINATIONS OF HYBRID MODULATION

b_{i-1}	b_i	Reference pulse modulation symbol $2\beta_j - 1$	Data pulse modulation symbol $2(\overline{\beta_j \oplus b_{\lfloor j/N_f \rfloor}}) - 1$	Phase difference between reference pulse & data pulse
0	0	-1	1	180°
0	1	-1	-1	0°
1	0	1	-1	180°
1	1	1	1	0°

waveforms, and their phase differences or polarities. The phase difference between the reference pulse and the data pulse is identical to the conventional TR system.

If the current bit is '0', then the phase difference between the reference pulse and the data pulse is always 180°, regardless of the value of the previous bit. If the current bit is '1', then the phase difference is 0°. Additionally, the sequence of pairs also contains the information about the previous bit in the polarity of the reference pulse. Again, this is illustrated in Table I, where the reference pulse in each pair has a $+/-$ polarity that indicates the value of the previously encoded bit.

Clearly, a TR receiver can demodulate this transmitted signal. The signal can also be demodulated by a coherent TH receiver with an improved performance compared to the coherent reception of conventional TR signals. The performance gain comes from the fact that information is encoded in both the reference pulses and the data pulses (see Table I). Thus, the coherent TH receiver can take advantage of the memory encoded in the reference pulses to improve performance.

Therefore, this hybrid modulation enables the use of both coherent and TR receivers in the same network. The choice of receiver can be based on considerations such as performance target, implementation cost, and desired radio frequency (RF) coverage area.

B. Alternative Interpretation and Receiver Structure

In the following, we give another interpretation of the modulation format, which also leads to the proposed receiver structure. During each symbol period, a sequence of N_f pulse pairs is transmitted. The pair in each frame consists of two pulses, each with a polarity depending on the current and previous bits transmitted. There are four possible combinations of pairs:

$$s_0(t) = \alpha(-1 \cdot p(t) + 1 \cdot p(t - T_d)) \tag{4a}$$
$$s_1(t) = \alpha(-1 \cdot p(t) - 1 \cdot p(t - T_d)) \tag{4b}$$
$$s_2(t) = \alpha(1 \cdot p(t) - 1 \cdot p(t - T_d)) \tag{4c}$$
$$s_3(t) = \alpha(1 \cdot p(t) + 1 \cdot p(t - T_d)) \tag{4d}$$

where the coefficient $\alpha = \frac{1}{\sqrt{2N_f E_p}}$ with E_p being the energy per pulse and N_f being the number of pulse pairs in a symbol normalizes the energy of the transmitted symbols. These signals can be represented by vectors as

$$s_0 = [-1 \quad 1] \tag{5a}$$
$$s_1 = [-1 \quad -1] \tag{5b}$$
$$s_2 = [\ 1 \quad -1] \tag{5c}$$
$$s_3 = [\ 1 \quad 1]. \tag{5d}$$

Therefore, the transmitted signal can also be described as follows. During each symbol period, the transmitter transmits a sequence of N_f pairs. The four possible pairs are given by Eq. (4). Optional polarity scrambling could be applied to the pairs to smooth the spectrum.

The above interpretation leads to a new improved coherent receiver structure. It becomes clear that the hybrid scheme provides a modulation format with memory, which can normally be represented by using a trellis diagram. Additionally, the transmitted signals are two-dimensional because two orthogonal basis functions $\Psi_0(t) = \alpha p(t)$ and $\Psi_1(t) = \alpha p(t - T_d)$ are used to represent the pairs.

Fig. 1(b) shows the trellis diagram describing the modulation. The trellis has two states, where state '0' represents a previous bit '0', and state '1' represents a previous bit '1'. Branches of the trellis indicate possible transitions. The branches are labeled with the value of the current input bit and the vector representation of the transmitted pair. For example, if the current state is '0' and a bit '1' is to be transmitted, then a transition to state '1' occurs, and pair $s_1 = [-1 \ -1]$ is transmitted. A MLSD detector determines the most probable path through the trellis for a given sequence of observations. Methods that approximate the MLSD detector, such as Viterbi decoding [25], can also be used.

Compared with an uncoded BPSK signal, there is a 3 dB loss when a coherent receiver is used to demodulate a conventional TR signal, since the reference pulse is non-information bearing and has to be simply "thrown away". If we denote ε as the bit energy, a BPSK signal constellation $\{\pm\sqrt{\varepsilon}\}$ and a conventional TR signal constellation $\{\pm\sqrt{\varepsilon/2}\}$ (ignoring the reference pulse) have Euclidean distances of $d_0 = 2\sqrt{\varepsilon}$ and $d_1 = \sqrt{2\varepsilon}$, respectively. Now let us examine the free Euclidean distance of the trellis shown in Fig. 1(b). By viewing the hybrid trellis modulation as a systematic convolutional encoding or a TCM, the minimum Euclidean distance is $\sqrt{d_0^2 + d_1^2} = \sqrt{6\varepsilon}$ between any two signal paths that leave one state and re-enter the same state. This clearly indicates that this trellis modulation not only compensates the 3 dB loss due to reference pulses in TR signaling but also gives an additional coding gain of about 1.76 dB compared with uncoded BPSK signaling. The trellis decoding does not impose a significant complexity increase for demodulation since it is only a very simple two-state trellis.

III. ENHANCED HYBRID MODULATION WITH ITERATIVE DECODING

A. Iterative Decoding

In practical communication systems, FEC codes are often used before digital modulation. For many applications, one simple FEC encoder may not be powerful enough, and a serial or parallel concatenation of two or more FEC codes with iterative decoding could be used to further improve the error-correction capability at the cost of higher hardware complexity [25], [26].

In heterogeneous networks, an FEC is usually required in order to ensure sufficiently low BER for TR receivers, which do not "see" the TCM described above. If such an FEC is used, then it also has beneficial effects on the coherent
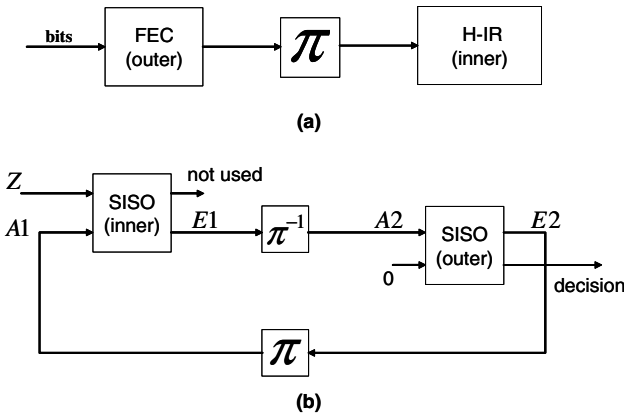
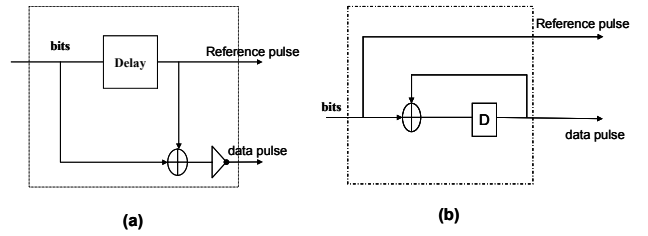Fig. 2. (a) Modified encoder structure; (b) Iterative decoding structure for hybrid modulation with FEC.

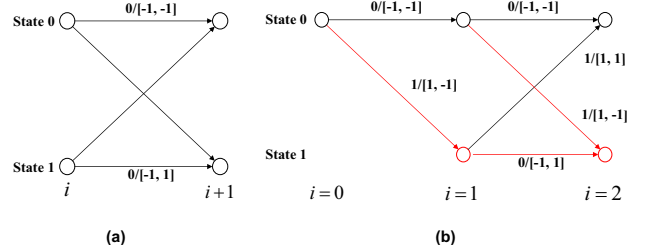Fig. 3. (a) The basic hybrid modulation; (b) The improved recursive hybrid modulation.

Fig. 4. (a) Trellis representation of the new recursive hybrid modulation; (b) An example on decoding the recursive modulated signals by TR receiver.

receivers: with only one FEC encoder, the proposed new hybrid scheme allows the implementation of powerful iterative decoding. Because the proposed modulation format already has memory and can be illustrated as a form of TCM, the hybrid modulation itself acts as an inner encoder. By simply adding one FEC code as an outer encoder, we can implement the iterative decoding. Because only one FEC encoder is required, the additional encoding hardware cost is minimal and the effective inner encoding does not reduce the data rate further.

Fig. 2 shows the block diagram of the improved encoder and the iterative decoder. In Fig. 2(a), information bits are FEC encoded before signal modulation and then passed through an interleaver (e.g., a pseudo-random interleaver) to randomize burst errors in the decoding stage. The iterative decoder consists of an inner decoder and an outer decoder, both are soft-input soft-output (SISO) decoders. A SISO decoder [19] is a four-port device that accepts the reliability information, or the corresponding probability distributions, of the information and encoded symbols as inputs, and outputs the updated reliability information based on the code constraints.

In Fig. 2(b), the inner SISO decoder is simply a maximum *a posteriori* probability (MAP) or maximum likelihood (ML) demodulator based on the trellis modulation, which incurs little extra complexity. The soft input of the coded symbol Z comes from the coherent rake detection, and the soft input of the information symbol $A1$ is the de-interleaved feedback from $E2$ at the outer decoder output. In the binary case, a common metric to represent the *a posteriori* probability is the log-likelihood ratio (LLR) defined as

$$L(\Delta) \triangleq \ln \frac{P\{\Delta = +1 | \text{inputs}\}}{P\{\Delta = -1 | \text{inputs}\}} \qquad (6)$$

where Δ is the decoder output and 'inputs' refers to all the decoder inputs.

One example of algorithms for use in the decoders is the modified Bahl, Cocke, Jelinek, Raviv (BCJR) algorithm [19], [27]. The rest of the decoding procedure follows the conventional iterative decoding algorithm of serially concatenated codes [19]. The outer FEC code can be selected according to the desired balance between complexity and performance.

B. A New Recursive Modulation

It is well known that recursive systematic convolutional (RSC) codes, when used as inner constituent code in concatenated coding along with iterative decoding, give far better error performance than their nonrecursive counterparts. From the output of the hybrid modulator and its associated trellis shown in Fig. 1, one can recognize this as a systematic convolutional encoding, i.e., the current bit/symbol is always present in the polarity of the reference pulse. However, the encoder is nonrecursive.

We therefore introduce a variant of the hybrid modulation of Section II that leads to a recursive systematic encoding, and is thus better suited to take advantage of the iterative decoding. This can be achieved by modifying the transmitter shown in Fig. 1(a) with the addition of a feedback line from the output of the delay element. The hybrid modulator and the recursive version are shown in Fig. 3. Similar to Eq. (2), the transmitted signal for this case is expressed as

$$s_{TX}(t) = \sqrt{\frac{E_s}{2N_f}} \sum_{j=-\infty}^{\infty} d_j \left[(2b_{\lfloor j/N_f \rfloor} - 1) p(t - jT_f - c_j T_c) \right.$$
$$\left. + \left(2\gamma_{\lfloor j/N_f \rfloor} - 1 \right) p(t - jT_f - c_j T_c - T_d) \right] \qquad (7)$$

where γ is given by

$$\gamma_{\lfloor j/N_f \rfloor} = b_{\lfloor j/N_f \rfloor} \oplus \gamma_{\lfloor j/N_f \rfloor - 1}. \qquad (8)$$

The modulator shown in Fig. 3(b) may be viewed as a new $\frac{1}{2}$-rate convolution encoder described by the generator polynomial $[1, \frac{D}{1+D}]$, where the denominator $1+D$ represents the feedback line. The corresponding new trellis is shown in Fig. 4(a). If the two output bits are used to encode the reference and data pulses as described in Section II, apparently a coherent receiver still works as before. Additionally, it achieves the performance gain by using a RSC code as the inner constituent code.

When using the recursive version of the hybrid modulation, the phase difference in a pulse pair does not depend on the

TABLE II
STATE AND PULSE COMBINATIONS OF RECURSIVE HYBRID
MODULATION

Trellis state	Phase difference between previously received pulse pair	Current bit	Phase difference between currently received pulse pair
0	0°	0	0°
0	0°	1	180°
1	180°	0	180°
1	180°	1	0°

Fig. 5. EXIT chart analysis of hybrid modulation schemes.

current input bit anymore. Instead, it only depends on the state transition. At first glance, one might have the impression that consequently, a trellis decoding is needed in the TR receiver. The increased complexity might be undesirable for simple TR receivers. After examining the new trellis in Fig. 4(a), however, we find that we can implement a symbol-by-symbol detection procedure, which does not require a sequence detector.

Fig. 4(b) illustrates the decoding procedure. Without loss of generality, we assume that decoding always starts with state '0'. At time $i = 2$, looking at the both branches entering state '0', the phase difference between pulse pairs are found to be the same, indicating that the path selection up to time $i = 1$ solely depends on the phase difference detected at that step. The situation is the same if we look at the branches entering state '1' at time $i = 2$. Thus, there is no need for decoding path memory or trace back. For example, at time $i = 1$, we know the previous state is '0'. Then as long as the phase difference is known to be 0° or 180° at time $i = 1$, the transmitted bit can be demodulated as '0' or '1' and the state changes to '0' or '1'. After the state at $i = 1$ is known, then the same procedure is applied to demodulate the next bit, and so on. Although the demodulation depends on the trellis state besides the phase difference in the received pulse pair, a detected phase difference of 180° always leads to the next state '1', regardless of the previous state. To summarize, there is no error propagation, which has been verified by using simulation, so that sequence detectors are not necessary for TR receivers. The state and pulse combinations are shown in Table II.

Again, the choice of receiver structure can be based on considerations of performance, implementation cost, and the desired RF coverage area.

IV. EXIT CHARTS OF THE HYBRID MODULATIONS

The major part of the iterative decoding procedure is an algorithm in each component decoder that computes the *a posteriori* probability of the information symbols, or more generally a reliability value for each information symbol. By exchanging the reliability information between decoders, each decoder exploits the redundant information that is not from itself to improve the decoding performance. In contrast to the *a priori* channel observation, which is intrinsic to the iterative decoding process, the original concept of *extrinsic information* was introduced in [20] to identify the component of the reliability value, which depends on the redundant information introduced by the considered constituent code.
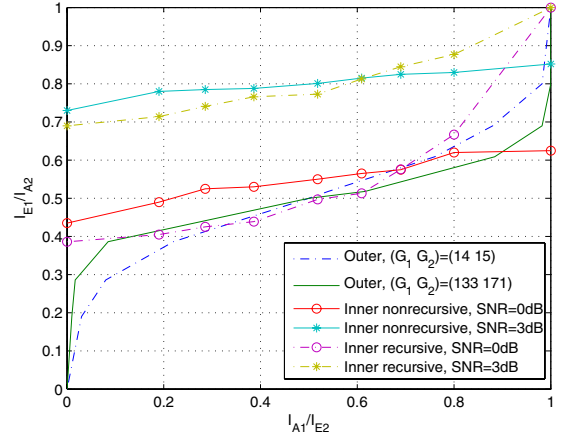
EXIT charts provide a visual tool to study the convergence behavior of parallel or serially concatenated codes [21], [22]. The idea is to predict the behavior of the iterative decoder by solely looking at the input/output relations of individual constituent decoders. Mutual information, a quantity that measures the mutual dependence of two variables, is used to describe the flow of extrinsic information through the SISO decoder.

Fig. 5 compares the transfer characteristics of different outer FEC codes and inner coded modulation methods. I_{A1} and I_{E1} represent, respectively, the input and output mutual information of the inner modulation, while I_{A2} and I_{E2} represent those of the outer FEC code. For the inner constituent code in a serial concatenation, the output mutual information I_{E1} can be viewed as a function of the input mutual information I_{A1} and the SNR E_b/N_0: $I_{E1} = F_1(I_{A1}, E_b/N_0)$. For the outer constituent code, I_{E2} only depends on I_{A2} and has no relation with E_b/N_0: $I_{E2} = F_2(I_{A2})$. During the decoding process as shown in Fig. 2(b), the extrinsic soft output $E1$ of the inner decoder becomes the *a priori* input $A2$ of the outer decoder, which then feeds back its output $E2$ as *a priori* input $A1$ of the inner decoder. So the axes are swapped for inner and outer codes: for inner modulation, I_{A1} is on the horizontal axis and I_{E1} is on the vertical axis; but for the outer code, the two axes are interchanged. The details about how to read an EXIT chart can be found in [21], [22].

In the EXIT chart analysis of the hybrid modulation scheme shown in Fig. 5, the curves of the outer FEC codes includes two $\frac{1}{2}$-rate convolutional codes of different constraint lengths (CL), which are represented by smooth lines (lines without marks). One is $CL = 7$ with generator polynomial $(G_1\ G_2) = (133\ 171)$ in octal, and the other is $CL = 4$ with generator polynomial $(G_1\ G_2) = (14\ 15)$. A shorter code memory tends to result in a steeper curve.

On the other hand, the inner modulation methods apparently play a more important role on the iterative decoding performance. Their transfer characteristics at different E_b/N_0 values are shown by lines with marks in Fig. 5. The solid lines show the transfer characteristics of the nonrecursive hybrid modulation while the dashed lines show those of the recursive hybrid modulation.

Although the solid lines with marks have higher mutual information at $I_{A1} = 0$, which means better bit-error rate (BER) after the first round of decoding, they are very flat and do not reach the point $(I_{A1}, I_{E1}) \approx (1, 1)$, which causes convergence problems at low BER after multiple iterations. The flatness of the line also indicates that decoding converges after a few iterations so that many decoding iterations are unnecessary, which will be verified by using simulation results in the next section. At low E_b/N_0 values, the marked dashed line crosses with the curves of the outer codes very early so that the decoding only converges to a point where mutual information is low, resulting in a decoding performance of the recursive modulation that is worse than the solid lines of the nonrecursive modulation. However, at high E_b/N_0 values, the dashed line reaches the point $(I_{A1}, I_{E1}) \approx (1, 1)$ and crosses with the outer codes at a point showing almost perfect mutual information. This indicates a great convergence capability at low BER of the enhanced recursive hybrid modulation with iterative decoding.

V. Numerical Results

In this section, we obtain simulation results that compare the different modulation options proposed, as used alone or in combination with a convolutional FEC code. For comparison, uncoded and convolutionally coded BPSK systems were also simulated under the same channel environment, processing gain, time hopping, and polarity scrambling sequences.

In all simulations, we used a carrier-modulated, truncated root-raised-cosine (RRC) pulse with a roll-off factor 0.25 as the UWB pulse shape $p(t)$ and the 10-dB signal bandwidth is 500 MHz. Because signal modulation compatible to both the TR and the coherent rake receivers has attracted significant interests from IEEE 802.15.4a task group (TG), we adopt the channel model from this group [11], which is generated from a large amount of measurements in different communication environments such as residential, office, industry, and outdoor, covering the frequency range from 2 GHz to 10 GHz. In this paper, for all simulations over multipath fading channels, the channel impulse response model in non-line-of-sight (NLOS) industrial environments (Channel model 8) from [11] is adopted, since it is the most challenging one due to its large multipath dispersion. Perfect channel knowledge is assumed at the receiver. The chip duration is set to $T_c = 4$ns, and the pulse pair spacing T_d and the guard time T_g are 20ns. The TH sequence is constructed from the algorithm proposed in [28] with $N_{TH} = N_f = 11$ and $T_f = 88$ns.

When a TR receiver is used with the proposed hybrid modulation scheme, the performance is the same as a conventional TR scheme with or without a single FEC code. Since performance of the conventional TR receivers have been analyzed extensively in literature [13]–[18], [29], simulation results are presented only for the coherent rake receiver. The rake receiver has 10 fingers to combine 10 strongest paths for each received symbol, and maximal ratio combining (MRC) is employed to collect multipath components.

A. Hybrid Modulation Without Coding

Firstly, we begin with a simple system that uses hybrid modulation without additional FEC coding. The data rate is
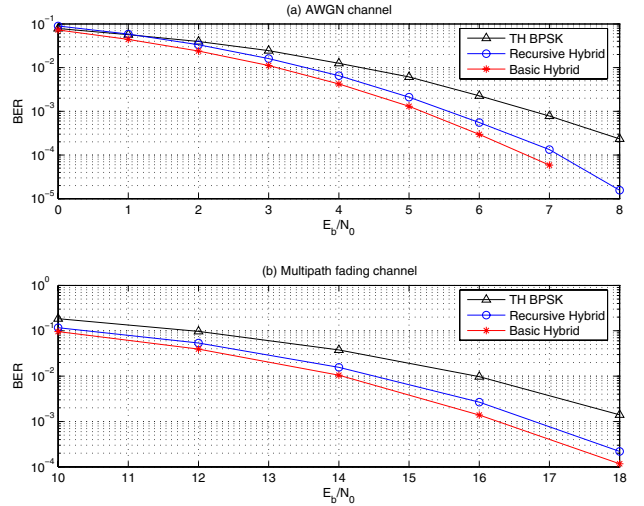

Fig. 6. BER versus SNR curves of uncoded hybrid with coherent rake receiver and BPSK modulation over (a) AWGN channels; (b) measured indoor industrial multipath fading channels.

set to be 1 Mbps. The rake MRC outputs are fed into a Viterbi detector and demodulated based on the trellis shown in Fig. 1(b).

Fig. 6(a) presents the system performance over additive white Gaussian noise (AWGN) channels and compares it with the theoretical performance of BPSK modulated system. The system performance over multipath fading channel is given in Fig. 6(b). For comparison, a BPSK modulated system is simulated with the same set of parameters (channel, processing gain, and time hopping and polarity scrambling sequences). The gain of hybrid modulation method over BPSK modulation is clearly observed.

B. Hybrid Modulation Concatenated With Convolutional Encoding

Now we compare different modulation options as they were used in combination with convolutional FEC codes. In these simulations, the data streams are encoded with the $\frac{1}{2}$-rate convolutional code $(G_1 \ G_2) = (14 \ 15)$, whose extrinsic information transfer characteristic has been shown in Fig. 5. The data rate is set to be 1 Mbps after FEC encoding, i.e., a user payload of 500 Kbps, which is a data rate of interest to the 802.15.4a TG. After encoding and random interleaving, the data are fed into the hybrid transmitter.

In this scheme, the rake MRC outputs are fed into the SISO decoder. In the adopted 802.15.4a channel model [11], 100 different channel realizations are given for each channel environment. As suggested by the 802.15.4a task group, in the simulation for each channel environment, 10 data packets of 256 bits/packet were simulated for each channel realization. Thus the interleaver size between the inner and outer codes is 512 bits.

Error performance curves of the nonrecursive and the recursive hybrid modulation schemes in AWGN environments are shown in Fig. 7 and Fig. 8, respectively, whereas the corresponding performances in multipath fading environments are shown in Figs. 9 and 10. We observed that the basic
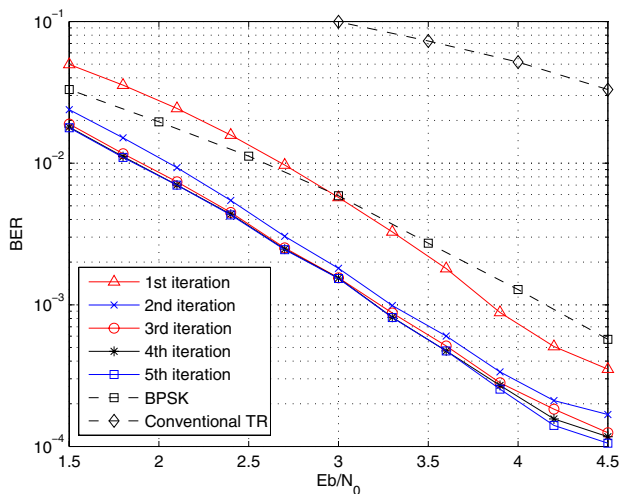
Fig. 7. BER versus SNR curves of the basic hybrid modulation scheme over AWGN channels: coherent receiver with iterative decoding.

Fig. 8. BER versus SNR curves of the recursive hybrid modulation scheme over AWGN channels: coherent receiver with iterative decoding.

nonrecursive hybrid modulation performs slightly better in the low-SNR region. At the high-SNR (low-BER) region, however, although the nonrecursive hybrid modulation gives better BER after the first round of decoding, the enhanced recursive hybrid modulation improves the system performance drastically after several decoding iterations. Because the interleaver size is limited, the system does not perform exactly as predicted from the EXIT chart shown in Fig. 5, which requires a very large interleaver size to achieve its potential. But the basic trend seen from the EXIT chart on decoding performance related to different inner/outer codes and different E_b/N_0 values matches well with the simulation results. Again, a BPSK modulated system and a system using conventional TR signaling are also simulated for comparison, with same FEC encoding, same channel, same processing gain, same time hopping and polarity scrambling sequences. The performance difference between the BPSK system and the hybrid system with no iterative decoding (i.e., after the first iteration) is not as big as the simple systems with no FEC. This is because BPSK demodulation gives more accurate soft output for further FEC decoding than hybrid modulation. However, BPSK systems cannot take advantage of the great power of iterative decoding. The system using conventional TR signaling suffers another 3 dB loss compared to the BPSK system.

VI. CONCLUSION

We have proposed a hybrid UWB modulation scheme that allows reception with good quality by both coherent and TR receivers. The key idea is to transmit information about previous information bits on the reference pulses of a TR modulation scheme, thus exploiting the energy contained in the reference pulses for coherent receivers, as well as introducing memory into the system. We then presented an enhanced version by concatenating the hybrid modulation with an FEC code for performance improvements through iterative decoding. Since only one additional FEC encoder is needed for the enhanced hybrid scheme, it adds very little extra hardware complexity to the encoder. We have analyzed the convergence behavior of the proposed enhanced hybrid scheme using the
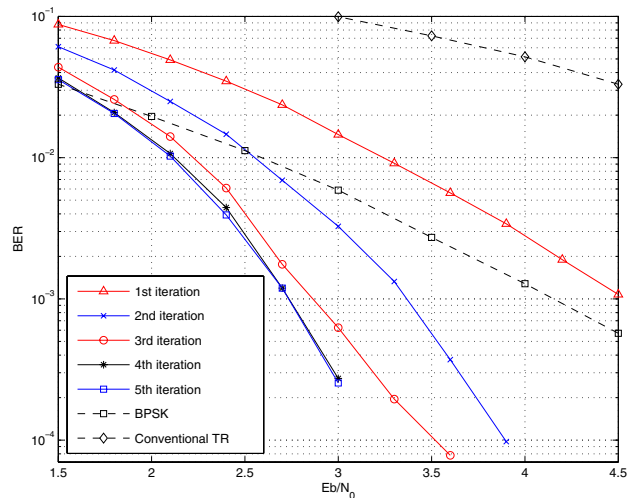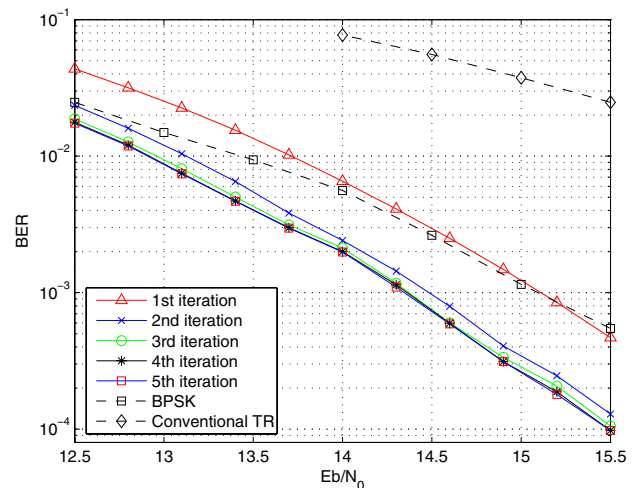

Fig. 9. BER versus SNR curves of the basic hybrid modulation scheme over measured indoor industrial multipath fading channels: coherent receiver with iterative decoding.

EXIT chart technique, which can also be used to optimize the choices of the constituent codes. Simulation results have shown a significant performance improvement by using iterative decoding and the proposed recursive hybrid modulation.

There are three options for receiver designs that work with our basic and recursive schemes, allowing flexible trade-offs between performance and complexity. The simplest TR receiver can be used for both modulation schemes in the usual way; an FEC encoding provides additional performance improvements. Coherent receivers with iterative decoding are favored for best performance. A compromise between performance and cost might be to use coherent receivers but not to implement iterative decoding. Such design flexibility is highly desirable for heterogenous networks like the ones envisioned for the IEEE 802.15.4a standard; for this reason, our modulation scheme is currently under consideration by this standardization body.
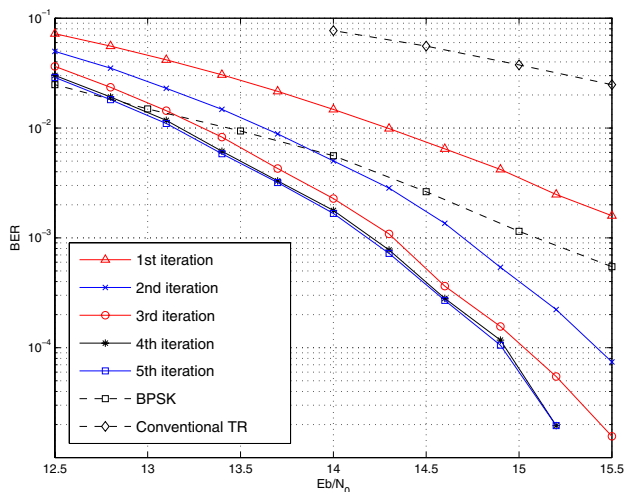
Fig. 10. BER versus SNR curves of the recursive hybrid modulation scheme over measured indoor industrial multipath fading channels: coherent receiver with iterative decoding.

REFERENCES

[1] M. G. diBenedetto, T. Kaiser, A. F. Molisch, I. Oppermann, C. Politano, and D. Porcino, Eds., *UWB Communications Systems: A Comprehensive Overview*. New York: Hindawi, 2006.

[2] R. C. Qiu, H. Liu, and X. Shen, "Ultra-wideband for multiple access communications," *IEEE Commun. Mag.*, vol. 43, pp. 80–87, Feb. 2005.

[3] L. Yang and G. B. Giannakis, "A general model and SINR analysis of low duty-cycle UWB access through multipath with narrowband interference and Rake reception," *IEEE Trans. Wireless Commun.*, vol. 4, pp. 1818–1833, July 2005.

[4] S. Gezici, Z. Tian, G. B. Giannakis, H. Kobayashi, A. F. Molisch, H. V. Poor, and Z. Sahinoglu, "Localization via ultra-wideband radios: A look at positioning aspects for future sensor networks," *IEEE Signal Processing Mag.*, vol. 22, pp. 70–84, July 2005.

[5] M. Z. Win and R. A. Scholtz, "Impulse radio: How it works," *IEEE Commun. Lett.*, vol. 2, pp. 36–38, Feb. 1998.

[6] M. Z. Win and R. A. Scholtz, "Ultra-wide bandwidth time-hopping spread-spectrum impulse radio for wireless multiple-access communications," *IEEE Trans. Commun.*, vol. 48, pp. 679–691, Apr. 2000.

[7] M. Z. Win and R. A. Scholtz, "On the energy capture of ultrawide bandwidth signals in dense multipath environments," *IEEE Commun. Lett.*, vol. 2, no. 9, pp. 245–247, Sep. 1998.

[8] S. Gaur and A. Annamalai, "Improving the range of UWB transmission using RAKE receivers," in *Proc. 53rd IEEE VTC*, Oct. 2003, vol. 1, pp. 597–601.

[9] A. F. Molisch, J. R. Foerster, and M. Pendergrass, "Channel models for ultrawideband personal area networks," *IEEE Trans. Wireless Commun.*, vol. 10, pp. 14–21, Dec. 2003.

[10] A. F. Molisch, K. Balakrishnan, C. C. Chong, D. Cassioli, S. Emami, A. Fort, J. Karedal, J. Kunisch, H. Schantz, and K. Siwiak, "A comprehensive model for ultrawideband propagation channels," *IEEE Trans. Antennas Propagat.*, submitted for publication.

[11] A. F. Molisch, K. Balakrishnan, C.-C. Chong, S. Emami, A. Fort, J. Karedal, J. Kunisch, H. Schantz, U. Schuster, and K. Siwiak, "IEEE 802.15.4a channel model - Final report," Document IEEE 802.15-04-0662-02-004a, 2005.

[12] D. Cassioli, M. Z. Win, A. F. Molisch, and F. Vatelaro, "Performance of selective Rake reception in a realistic UWB channel," in *Proc. IEEE ICC*, Apr. 2002, pp. 763–767.

[13] R. T. Hoctor and H. W. Tomlinson, "An overview of delay-hopped, transmitted-reference RF communications," *Technical Information Series*, GE Research and Development Center, pp. 1–29, Jan. 2002.

[14] J. D. Choi and W. E. Stark, "Performance of ultra-wideband communications with suboptimal receiver in multipath channels," *IEEE J. Select. Areas Commun.*, vol. 20, no. 9, pp. 1754–1766, Dec. 2002.

[15] K. Witrisal, G. Leus, M. Pausini, and C. Krall, "Equivalent system model and equalization of differential impulse radio UWB systems," *IEEE J. Select. Areas Commun.*, vol. 23, pp. 1851–1862, Sep. 2005.

[16] T. Q. S. Quek and M. Z. Win, "Analysis of UWB transmitted-reference communication systems in dense multipath channels," *IEEE J. Select. Areas Commun.*, vol. 23, pp. 1863–1874, Sep. 2005.

[17] S. Gezici, F. Tufvesson, and A. F. Molisch, "On the performance of transmitted-reference impulse radio," in *Proc. IEEE Globecom*, Nov. 2004, pp. 2874-2879.

[18] S. Zhao, H. Liu, and Z. Tian, "Decision directed autocorrelation receivers for pulsed ultra-wideband systems," *IEEE Trans. Wireless Commun.*, vol. 5, pp. 2175–2184, Aug. 2006.

[19] S. Benedetto, D. Divsalar, G. Montorsi, and F. Pollara, "Serial concatenation of interleaved codes: Performance analysis, design, and iterative decoding," *IEEE Trans. Inform. Theory*, vol. 44, no. 3, pp. 909–926, May 1998.

[20] C. Berrou and A. Glavieux, "Near optimum error correcting coding and decoding: Turbo-codes," *IEEE Trans. Commun.*, vol. 44, pp. 1261–1271, Oct. 1996.

[21] S. ten Brink, "Convergence behavior of iteratively decoded parallel concatenated codes," *IEEE Trans. Commun.*, vol. 49, no. 10, pp. 1727–1737, Oct. 2001.

[22] S. ten Brink, "Design of serially concatenated codes based on iterative decoding convergence," in *Proc. Int. Symp. Turbo Codes Related Topics*, Sep. 2000, pp. 319-322.

[23] P. V. Orlik, S. Zhao, and A. Molisch, "A hybrid UWB modulation design compatible for both coherent and noncoherent receivers," in *Proc. IEEE ICC*, June 2006, vol. 10, pp. 4741–4745.

[24] Y. P. Nakache and A. F. Molisch, "Spectral shape of UWB signals: Influence of modulation format, multiple access scheme and pulse shape," in *Proc. IEEE VTC-Spring*, Apr. 2003, vol. 4, pp. 2510–2514.

[25] J. G. Proakis, *Digital Communications*, 4th ed. New York: McGraw-Hill, 2001.

[26] A. F. Molisch, *Wireless Communications*. New York: IEEE Press-Wiley, 2005.

[27] L. R. Bahl, J. Cocke, F. Jelinek, and J. Raviv, "Optimal decoding of linear codes for minimizing symbol error rate," *IEEE Trans. Inform. Theory*, vol. 20, no. 2, pp. 284–287, Mar. 1974.

[28] R. A. Scholtz, P. V. Kumar, and C. J. Corrada-Bravo, "Signal design for ultra-wideband radio." in *Sequences and Their Applications-SETA'01*, T. Helleseth, P. Kumar, and K. Yang, Eds., pp. 72-87. London, U.K.: Springer, 2001.

[29] L. Yang and G. B. Giannakis, "Optimal pilot waveform assisted modulation for ultra-wideband communications," *IEEE Trans. Wireless Commun.*, vol. 3, no. 4, pp. 1236–1249, July 2004.

Shiwei Zhao received his bachelor degree in computer science from the University of Science and Technology of China (USTC), Hefei, China, in 1999, and his Ph.D degree in wireless communications from Oregon State University, Corvallis, Oregon, in 2006. From Jan. 2005 to June 2005, he had an internship at Mitsubishi Electric Research Lab (MERL), where he worked on proposal drafting to the IEEE 802.15.4a study group (low rate UWB systems). Since June 2006, he has been a wireless engineer with Trapeze Networks, where he is working on RF management. He has published journal and conference papers and filed two patent applications, and is co-inventor of several US and international patents.

Philip V. Orlik (S'97-M'99) was born in New York, NY in 1972. He received the B.E. degree in 1994 and the M.S. degree in 1997 both from the State University of New York at Stony Brook. In 1999 he earned his Ph.D. in electrical engineering also from SUNY Stony Brook.

He is currently a principal technical staff member at Mitsubishi Electric Research Laboratories Inc. located in Cambridge, MA. His primary research focus is on sensor networks, ad hoc networking and UWB. Other research interests include mobile cellular and wireless communications, mobility modeling, performance analysis, queueing theory, and analytical modeling.

Andreas F. Molisch (S'89-M'95-SM'00-F'05) received the Dipl. Ing., Dr. techn., and habilitation degrees from the Technical University Vienna (Austria) in 1990, 1994, and 1999, respectively. From 1991 to 2000, he was with the TU Vienna, becoming an associate professor there in 1999. From 2000-2002, he was with the Wireless Systems Research Department at AT&T (Bell) Laboratories Research in Middletown, NJ. Since then, he has been with Mitsubishi Electric Research Labs, Cambridge, MA, where he is now a Distinguished Member of Technical Staff. He is also professor and chairholder for radio systems at Lund University, Sweden.

Dr. Molisch has done research in the areas of SAW filters, radiative transfer in atomic vapors, atomic line filters, smart antennas, and wideband systems. His current research interests are measurement and modeling of mobile radio channels, UWB, cooperative communications, and MIMO systems. Dr. Molisch has authored, co-authored or edited four books (among them the recent textbook *Wireless Communications*, Wiley-IEEE Press), eleven book chapters, some one hundred journal papers, and numerous conference contributions.

Dr. Molisch is an editor of the IEEE TRANSACTIONS ON WIRELESS COMMUNICATIONS, co-editor of recent special issues on MIMO and smart antennas (in *J. Wireless Comm. Mob. Comp.*), and UWB (in IEEE JSAC). He has been a member of numerous TPCs, vice chair of the TPC of VTC 2005 spring, general chair of ICUWB 2006, TPC co-chair of Chinacom 2006, and TPC co-chair of the wireless symposium of Globecom 2006. He has participated in the European research initiatives "COST 231," "COST 259," and "COST273," where he was chairman of the MIMO channel working group. He was chairman of the IEEE 802.15.4a channel model standardization group, and is also chairman of Commission C (signals and systems) of URSI (International Union of Radio Scientists). Dr. Molisch is a Fellow of the IEEE and is the recipient of several awards.

Huaping Liu (S'95-M'97) received his B.S. and M.S. degrees from Nanjing University of Posts and Telecommunications, Nanjing, P.R. China, in 1987 and 1990, respectively, and his Ph.D. degree from New Jersey Institute of Technology, Newark, NJ, in 1997, all in electrical engineering. From July 1997 to August 2001, he was with Lucent Technologies, New Jersey. He joined the School of Electrical Engineering and Computer Science at Oregon State University in September 2001, and is currently an associate professor. His research interests include capacity and performance analysis of wireless networks, communication techniques for multiuser time-varying environments with applications to cellular and indoor wireless communications, ultra-wideband schemes, and MIMO OFDM systems.

Jinyun Zhang received her Ph.D. in electrical engineering from the University of Ottawa in 1991. Since 2001, Dr. Zhang has been the head and Senior Principal Technical Staff of digital communications and networking group at Mitsubishi Electric Research Laboratories (MERL). She is leading many new wireless communications and networking research projects that include UWB, ZigBee, wireless sensor network, MIMO, high speed WLAN, and next generation mobile communications. Prior to joining MERL she worked for Nortel Networks for more than 10 years, where she held engineering and management positions in the areas of digital signal processing, advanced wireless technology development and optical networks. Dr. Zhang is a Senior Member of the IEEE and an Associate Editor of the IEEE TRANSACTIONS ON BROADCASTING.